Developmental Cell, Vol. 3, 903–910, December, 2002, Copyright ©2002 by Cell Press

# The Retinoblastoma-Histone Deacetylase 3 Complex Inhibits PPARγ and Adipocyte Differentiation

**Lluis Fajas,[1,6] Viviane Egler,[1,5] Raphael Reiter,[1,5] Jacob Hansen,[2] Karsten Kristiansen,[2] Marie-Bernard Debril,[1] Stéphanie Miard,[1] and Johan Auwerx[1,3,4]**

[1]Institut de Génétique et de Biologie Moléculaire et Cellulaire
CNRS/INSERM/ULP
67404 Illkirch
France

[2]Department of Biochemistry and Molecular Biology
Odense University
5230 Odense
Denmark

[3]Institut Clinique de la Souris (ICS)
67404 Illkirch
France

## Summary

**The retinoblastoma protein (RB) has previously been shown to facilitate adipocyte differentiation by inducing cell cycle arrest and enhancing the transactivation by the adipogenic CCAAT/enhancer binding proteins (C/EBP). We show here that the peroxisome proliferator-activated receptor γ (PPARγ), a nuclear receptor pivotal for adipogenesis, promotes adipocyte differentiation more efficiently in the absence of RB. PPARγ and RB were shown to coimmunoprecipitate, and this PPARγ-RB complex also contains the histone deacetylase HDAC3, thereby attenuating PPARγ's capacity to drive gene expression and adipocyte differentiation. Dissociation of the PPARγ-RB-HDAC3 complex by RB phosphorylation or by inhibition of HDAC activity stimulates adipocyte differentiation. These observations underscore an important function of both RB and HDAC3 in fine-tuning PPARγ activity and adipocyte differentiation.**

## Introduction

One of the first events following hormonal induction of differentiation of preadipocytes is a reentry of these growth-arrested preadipocytes into the cell cycle. After several rounds of clonal expansion, these cells arrest again and undergo terminal adipocyte differentiation (reviewed in Fajas et al., 2001). Blocking cell cycle reentry with DNA synthesis inhibitors prevents adipocyte differentiation, suggesting that active cell cycle machinery is required for the differentiation process (Richon et al., 1997). The retinoblastoma protein RB, which is a negative regulator of the cell cycle, plays a dual role in adipocyte differentiation. During clonal expansion, RB plays a negative role by inhibiting reentry into the cell cycle of preadipocytes. Consequently, RB has been found to be hyperphosphorylated and, thus, inactive in these early stages of adipogenesis (Richon et al., 1997). In the later stages, RB positively regulates adipogenesis participating in the cell cycle exit required for terminal differentiation. Consistent with this is the observation that pRB inactivation, by SV40 large T antigen, inhibits adipogenesis (Higgins et al., 1996). Moreover, pRB-deficient fibroblasts fail to differentiate into adipocytes when properly stimulated (Chen et al., 1996b; Classon et al., 2000; Hansen et al., 1999). A second, positive role for RB in adipocyte differentiation is the consequence of its stimulatory effect on the transactivation by the proadipogenic C/EBPs, which is mediated via a direct protein-protein interaction (Chen et al., 1996b).

Since both PPARγ and RB are major regulators of cell proliferation and differentiation, a crosstalk between PPARγ and RB signaling might operate during adipocyte differentiation. We show here that RB recruits histone deacetylase 3 (HDAC3) to PPARγ target genes. Disruption of the PPARγ-RB-HDAC3 complex by phosphorylation of RB or inhibition of HDAC3 activity results in the activation of PPARγ, translating to an increase in adipogenesis.

## Results and Discussion

To analyze the effects of RB on adipogenesis, we compared the efficacy of RB+/+ or RB−/− MEFs to differentiate into adipocytes. A standard differentiation mixture (MDI) induced significant lipid accumulation, as assessed by Oil Red O staining, in RB+/+, but not in RB−/−, MEFs (Figure 1A). These differences were not the consequence of decreased expression of PPARγ (Figure 1B). Interestingly, when the PPARγ agonist rosiglitazone was added to the differentiation mix, a striking increase in lipid accumulation was observed in RB−/− MEFs, which now became even more pronounced than in rosiglitazone-treated RB+/+ cells (Figure 1A). Furthermore, the adipocyte-specific marker aP2 was more robustly induced in RB−/− than in RB+/+ MEFs after rosiglitazone (Figure 1B).

These data suggested that RB inhibited PPARγ activity and, hence, negatively regulates rosiglitazone-stimulated adipogenesis. This hypothesis was further tested by transient transfection experiments in RB−/− MEFs with PPARγ and RB expression vectors and a PPARγ-responsive luciferase reporter (PPRE-TK-Luc). A 7-fold induction of luciferase activity was observed upon transfection of PPARγ in the presence of rosiglitazone. This induction was significantly attenuated by cotransfection of RB (Figure 1C). To further demonstrate that RB negatively influences PPARγ activity, we used a Gal4-responsive luciferase reporter (UAS-TK-Luc) and a plasmid expressing a BD Gal4-PPARγ DE fusion protein, which contains the Gal4 DNA binding domain fused to the ligand binding domain (DE) of PPARγ. Cotransfection of BD Gal4-PPARγ DE with UAS-TK-Luc resulted in a 2-fold increase in luciferase activity, which was further

[4]Correspondence: auwerx@igbmc.u-strasbg.fr
[5]These authors contributed equally to this work.
[6]Present address: Endocrinologie Moléculaire et Cellulaire des Cancers, 60 rue Navacelles, 34090 Montpellier, France.

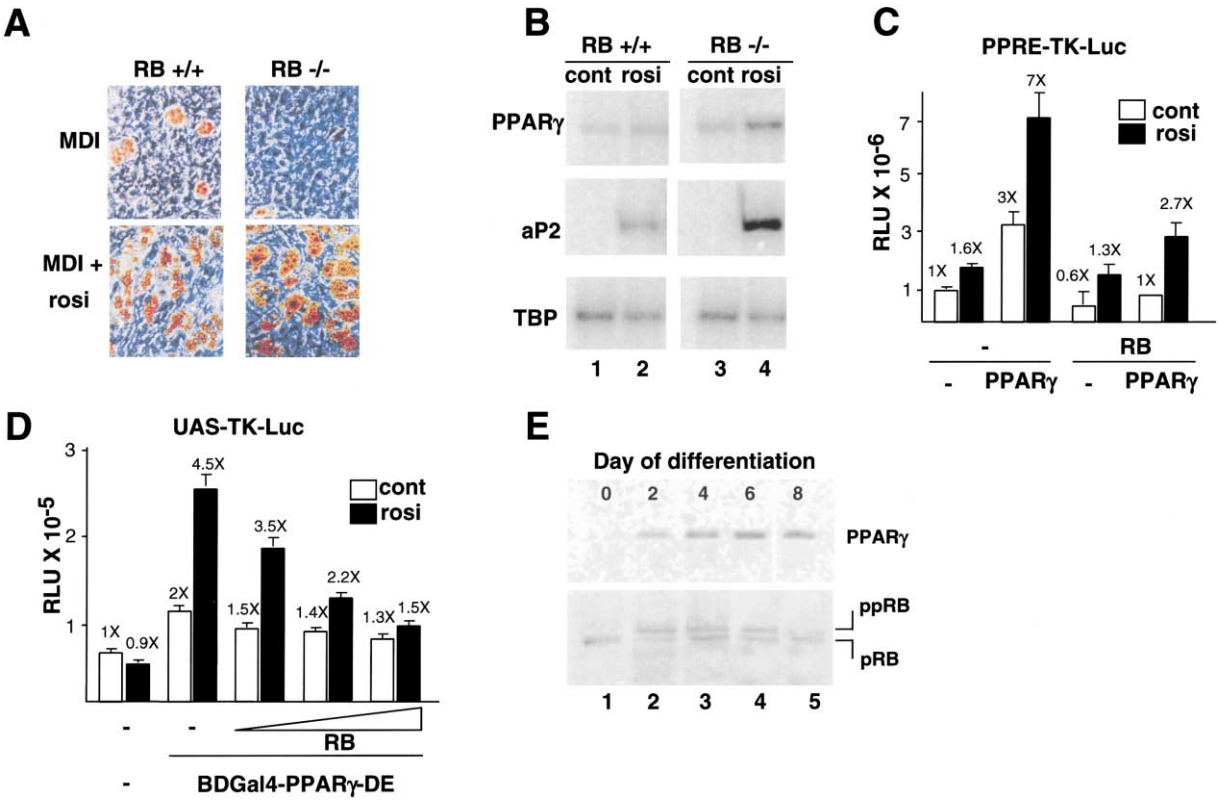


Figure 1. Rosiglitazone Enhances Adipocyte Differentiation in the Absence of RB

(A) Micrographs of Oil Red O-stained RB+/+ and RB−/− MEFs 10 days after the induction of differentiation. Cells in the upper panel were challenged with a standard adipogenic regimen (MDI). Cells in the lower panel were induced to differentiate with MDI, to which $10^{-6}$ M rosiglitazone (rosi) was added. In all future experiments the same concentration of rosiglitazone was used.

(B) Expression of adipocyte marker genes analyzed by multiplex RT-PCR in RB+/+ and RB−/− MEFs treated (rosi) or not (cont) with MDI in the presence of rosiglitazone for 3 days.

(C) Activity of the PPRE-TK-Luc reporter transfected in RB−/− MEFs with expression vectors for PPARγ, RB, or both together. Experiments were performed either in the absence (open bars) or presence of rosiglitazone (black bars). No effect on β-gal acivity was observed. Fold-induction relative to the basal condition is shown.

(D) Activity of the UAS-TK-Luc reporter transfected in RB−/− MEFs with an expression vector for a BD Gal4-PPARγ DE fusion protein alone or in combination with increasing amounts of an RB expression vector. The experiments were normalized for β-gal activity.

(E) Expression of PPARγ and RB during differentiation of 3T3-L1 cells into adipocytes was analyzed by immunoblotting. Phosphorylated RB (ppRB) is the slower-migrating band relative to hypophosphorylated RB (pRB).

enhanced up to 4.5-fold on addition of rosiglitazone (Figure 1D). Increasing concentrations of RB dose dependently decreased rosiglitazone-dependent PPARγ activity (Figure 1D), demonstrating that RB inhibits PPARγ.

Consistent with a negative role of RB during adipocyte differentiation, RB was phosphorylated between days 2 and 6 of 3T3-L1 differentiation (Figure 1E and Reichert and Eick, 1999). At day 8, when cells were fully differentiated, RB was mostly hypophosphorylated again. The presence of phosphorylated and, thus, inactive RB at a critical period during the differentiation process suggested that hypophosphorylated active RB negatively influences PPARγ activity. In line with this, other groups have previously reported the presence of hyperphosphorylated RB between days 1 and 5 (Hansen et al., 1999; Shao and Lazar, 1997), a time when maximal PPARγ activity is required to boost adipocyte differentiation, and the reoccurence of hypophosphorylated RB in fully differentiated adipocytes (between days 6 and 8) (Hansen et al., 1999; Shao and Lazar, 1997), when PPARγ activity is no longer required. Interestingly, not only PPARγ activity, but also PPARγ expression, is reduced in fully differentiated adipocytes, suggestive of a less important role of PPARγ at that stage (Rosenbaum and Greenberg, 1998).

To test whether the inhibition of PPARγ activity in the presence of RB was the consequence of an interaction between PPARγ and RB, nuclear extracts from rosiglitazone-treated 3T3-L1 cells during (day 4) or after (day 8) differentiation into adipocytes were immunoprecipitated with an anti-PPARγ antibody. A 110 kDa protein was recognized in the immunoprecipitates by an anti-RB antibody, indicating that RB interacted directly in vivo with PPARγ after adipocyte differentiation (Figure 2A, lane 5, day 8). This RB-PPARγ complex was not present in actively differentiating cells (Figure 2A, lane 4, day 4). According to the transfection data in Figures 1C and 1D, the lack of interaction of PPARγ with RB at day 4 of differentiation should increase PPARγ activity. In line with this hypothesis, the expression of lipoprotein lipase (LPL), a PPARγ target gene, was induced by rosiglitazone in differentiating 3T3-L1 cells (Figure 2B, day 4), but not in fully differentiated 3T3-L1 adipocytes (Figure

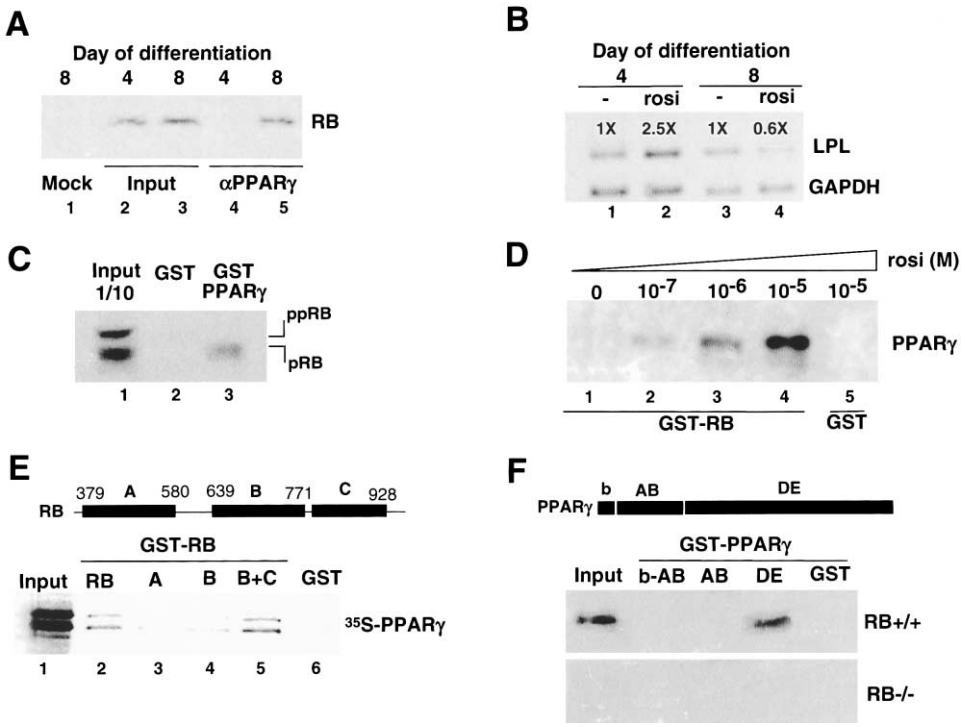


Figure 2. PPARγ Interacts with RB

(A) Coimmunoprecipitation of PPARγ and RB from 3T3-L1 cells during (day 4) or after adipocyte differentiation (day 8) in the presence of rosiglitazone. Extracts are immunoprecipitated with either an anti-PPARγ antibody (αPPARγ, lanes 4–5) or preimmune serum (Mock, lane 1) and revealed by an anti-RB antibody. One fifth of the input is shown as a control (lanes 2 and 3).

(B) Semi-quantitative RT-PCR showing expression of the mouse LPL and GAPDH mRNA in either differentiating (day 4) or differentiated (day 8) 3T3-L1 cells. Relative expression of LPL mRNA in rosiglitazone-treated versus untreated cells is indicated as fold induction.

(C) GST pull-down assay showing the interaction of PPARγ with hypophosphorylated RB. Nuclear extracts from rosiglitazone-treated RB+/+ MEFs were incubated with Sepharose-bound GST-PPARγ fusion protein or GST alone. Bound proteins were immunoblotted with an anti-RB antibody, which recognizes all forms of RB. Hypo- (pRB) and hyperphosphorylated (ppRB) RB is indicated. One-tenth of the input demonstrated the presence of both forms of RB.

(D) GST-pull down assay showing ligand-dependent PPARγ-RB interaction. GST alone or GST-RB protein (aa 379–928) was incubated with the hPPARγ DE protein (residues 203–477) in the presence of increasing amounts of rosiglitazone. Bound protein was visualized with an anti-PPARγ antibody.

(E) GST pull-down assays with in vitro-translated $^{35}$S-radiolabeled PPARγ protein and the indicated GST-RB constructs or GST alone. A scheme of the distinct RB domains is shown.

(F) GST pull-down assays with nuclear extracts from RB+/+ or RB−/− MEFs treated with rosiglitazone for 3 days and GST-PPARγ fusion proteins or GST alone. Proteins were immunoblotted with an anti-RB antibody. A scheme of the domain structure of PPARγ is shown.

2B, day 8). This result appears to contradict previous data from our laboratory demonstrating an induction of LPL mRNA in both adipocyte cell lines and adipose tissue in response to rosiglitazone (Schoonjans et al., 1996). In this last study, LPL expression was, however, not analyzed in fully differentiated cells, but in differentiating cells (Schoonjans et al., 1996). Furthermore, in adipose tissue, which is heterogeneous in nature and composed of adipocytes, preadipocytes, and stromal cells, the PPARγ-mediated stimulation of LPL expression in subset of cells (i.e., preadipocytes) would mask any repressive effect in mature adipocytes.

Inactivation of RB by phosphorylation could explain, at least in part, the decrease of PPARγ-RB interaction and, therefore, the increase in PPARγ activity required for adipocyte differentiation. To prove that PPARγ interacts only with the hypophosphorylated form of RB, GST-PPARγ DE fusion protein was incubated with nuclear extracts from rosiglitazone-treated RB+/+ MEFs, and the precipitates were immunoblotted with an anti-RB antibody (Figure 2C). RB+/+ MEFs contained both hyper- (slow-migrating) and hypophosphorylated (fast-migrating) RB, but only the fast-migrating form of RB was retained by GST-PPARγ (Figure 2C), demonstrating that PPARγ interacts preferentially with hypophosphorylated RB.

We also determined whether ligand binding of PPARγ could influence the interaction between PPARγ and RB. While very little, if any, PPARγ interacted with GST-RB in absence of ligand, binding of PPARγ to GST-RB was dose dependently enhanced by rosiglitazone (Figure 2D). The domains in RB and PPARγ that interact were then mapped (Figures 2E and 2F). Using in vitro-translated $^{35}$S-radiolabeled PPARγ2 and GST fusion proteins containing distinct domains of RB, we demonstrated that PPARγ interacted with GST-RB fusion proteins containing either the three pockets (A, B, and C) or pockets B and C (Figure 2E, lanes 2 and 5). PPARγ interacted weakly, or not at all, with the B and A pockets of RB, respectively (Figure 2E, lanes 3 and 4). Likewise, different GST-fusion proteins containing either exon b and the AB domain (b-AB), the AB domain (AB), or the DE

domain of PPARγ were incubated with nuclear extracts from confluent RB+/+ or RB−/− MEFs, and bound proteins were immunoblotted with an anti-RB antibody (Figure 2F). RB was only retained by the GST-PPARγ DE fusion protein in RB+/+ MEFs (Figure 2F, top panel), which is coherent with the ligand-dependence of the interaction between PPARγ and RB (Figure 2D).

It is well established that hypophosphorylated RB binds to the cell cycle regulator E2F and either blocks activation of E2F target genes or actively represses transcription through recruitment of histone deacetylases (HDACs) (Brehm et al., 1998; Magnaghi-Jaulin et al., 1998). We next tested whether repression of PPARγ activity by RB could be mediated by recruitment of histone deacetylases (HDACs) in immunoprecipitation studies. Protein extracts from COS cells transfected with expression vectors for PPARγ, Flag-HDAC3, and RB were immunoprecipitated with either anti-PPARγ or anti-Flag antibodies. PPARγ immunoprecipitates contained both HDAC3 and RB (Figure 3A). Similarly, Flag (HDAC3) immunoprecipitates contained RB and PPARγ (Figure 3A), strongly suggesting that PPARγ, RB, and HDAC3 are part of the same protein complex in the cell.

To obtain further proof of the crucial role of RB in this complex, nuclear extracts from rosiglitazone-treated RB+/+ or RB−/− MEFs were analyzed by GST pull-down assays with a GST-PPARγ DE fusion protein. Only in RB+/+ MEFs, but not in RB−/− MEFs, HDAC3 was retained by GST-PPARγ (Figure 3B). HDAC1, 2, 4, or 5 could not be detected when specific antibodies were used (data not shown). To assess that HDAC3 was functional in this complex, proteins bound either to the GST or GST-PPARγ were incubated with histone H4 that had been acetylated on Lys 9. Using an anti-acetylated histone H4 (Lys 9) antibody, we demonstrated that histone H4 was specifically deacetylated by proteins bound to the GST-PPARγ, but not to GST itself (Figure 3C). When the HDAC inhibitor, 4-phenyl butyrate (4PB), was included in the incubation, acetylated histone H4 remained detectable (Figure 3C). No deacetylation activity was present in extracts from RB−/− MEFs, suggesting that the HDAC activity was dependent on the presence of RB (data not shown).

To demonstrate that this PPARγ-RB-HDAC3 complex occupied PPARγ-dependent promoters in vivo, we performed a chromatin immunoprecipitation (ChIP) analysis of the LPL promoter in both RB+/+ U2OS and RB−/− SaOS cells. A 200 bp fragment of the human lipoprotein lipase (LPL) promoter, containing the binding site of PPARγ (Schoonjans et al., 1996), was amplified by PCR when anti-RB, anti-PPARγ, or anti-HDAC3 antibodies were used to immunoprecipitate chromatin from rosiglitazone-treated U2OS cells (Figure 3D). Although PPARγ was present, HDAC3 was not detected on the LPL promoter in the SaOS cells (Figure 3D). Since HDAC3 is expressed in SaOS cells (data not shown), these data further support the hypothesis that RB is required to recruit HDAC3 to PPARγ target genes.

To prove that the attenuation of PPARγ activity by RB was mediated by HDACs, we tested the effects of the HDAC inhibitor trichostatin A (TSA) in transfection experiments in RB−/− MEFs. Addition of suboptimal concentrations of TSA ($10^{-7}$ M) to RB−/− MEFs transfected with PPARγ had a minimal effect on PPARγ activation by rosiglitazone (Figure 3E). Cotransfection of RB with PPARγ attenuated the induction of the reporter by rosiglitazone. Combination of rosiglitazone with TSA, however, abrogated this inhibitory effect of RB on PPARγ, thereby mimicking the situation where RB is absent (Figure 3E). Similar results were obtained with 4PB (data not shown). Furthermore, coincubation of confluent and serum-starved RB+/+ U2OS cells with rosiglitazone and TSA resulted in a 2.5-fold induction of LPL mRNA, whereas no induction in LPL mRNA levels was observed upon treatment with rosiglitazone or TSA alone (Figure 3F). Importantly, confluent and serum-starved U2OS cells contain hypophosphorylated and, thus, active RB (data not shown), which is nonpermissive for the induction of LPL expression (see also Figure 2C). Interestingly, treatment of TSA alone had a repressive effect on the LPL expression (Figure 3F, lane 3). Whether this TSA-mediated repression of LPL has any physiological implication awaits further study. In contrast to the data in U2OS cells, rosiglitazone by itself increased LPL mRNA levels by 2-fold in RB-deficient SaOS cells (data not shown), a situation similar to that observed in U2OS cells treated with TSA and rosiglitazone.

Our results so far suggest that RB recruits HDACs to PPARγ target genes to repress transcription. To obtain experimental evidence of this, we performed another ChIP in U2OS cells (Figure 3G). No acetylated histone H4 was immunoprecipitated complexed to the LPL promoter when U2OS cells were incubated with rosiglitazone alone. PPARγ and HDAC3 were, however, present on the LPL promoter under these conditions, suggesting that the PPARγ-RB-HDAC3 complex silenced LPL expression (Figure 3G). More HDAC3 was present upon rosiglitazone treatment relative to control cells, consistent with the ligand dependence of RB recruitment to PPARγ. In contrast, treatment of U2OS cells with both TSA and rosiglitazone resulted in the disappearance of HDAC3 from the LPL promoter. This loss of HDAC3 was concomitant with histone H4 acetylation, indicative of promoter activation and consistent with the increase in LPL mRNA seen in these U2OS cells stimulated with rosiglitazone and TSA (Figure 3F, lane 4). Disruption of the HDAC3 complex by TSA was furthermore demonstrated by GST pull-down assays using GST or GST-PPARγ proteins and cell extracts from COS cells transfected with HDAC3 and RB expression vectors. Western blot analysis demonstrated that HDAC3 was among the proteins retained by GST-PPARγ (Figure 3H). More HDAC3 was retained when cells were incubated with rosiglitazone, whereas rosiglitazone in the presence of TSA resulted in the disappearance of HDAC3 from the GST-PPARγ complex (Figure 3H). This result is consistent with a previous report indicating that HDAC inhibitors disrupted an Sp1/Sp3/HDAC1 complex on the insulin-like growth factor binding protein 3 (IGFBP-3) promoter (Choi et al., 2002).

We next evaluated the effects of HDAC inhibition on 3T3-L1 adipocyte differentiation. Four days after incubation with the MDI differentiation mix, 3T3-L1 cells did not yet accumulate significant amounts of lipids, as evidenced by the absence of Oil Red O staining (Figure 4A, first panel). In contrast, 3T3-L1 cells incubated with

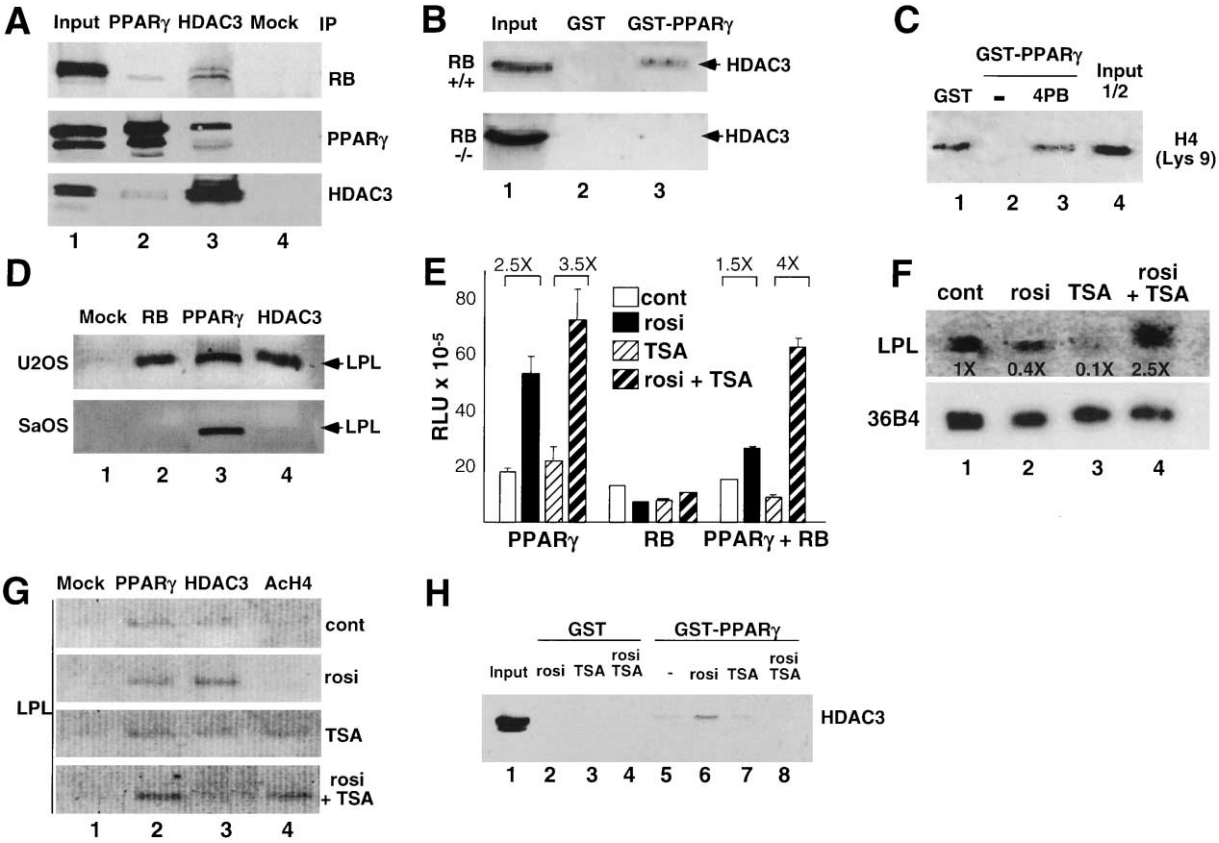


Figure 3. PPARγ Activity Is Modified by RB, which Recruits HDAC3 to PPARγ

(A) Immunoprecipitation assay showing interaction between HDAC3, RB, and PPARγ. Extracts from COS cells transfected with Flag-HDAC3, PPARγ, and RB were immunoprecipitated with anti-PPARγ (lane 2), anti-Flag-HDAC3 (lane 3), or preimmune serum (Mock, lane 4) or directly analyzed for the presence of RB, PPARγ, and Flag-HDAC3 (Input, lane 1). Western blot analysis revealed the presence of RB (upper panel), PPARγ (middle panel), or HDAC3 (lower panel) in both PPARγ and Flag-HDAC immunoprecipitates.

(B) GST pull-down assay showing the presence of HDAC3 in the PPARγ-RB complex. Nuclear extracts of rosiglitazone-treated RB+/+ or RB−/− MEFs were incubated with Sepharose-bound GST-PPARγ or GST alone. Bound proteins were immunoblotted with an anti-HDAC3 antibody. One-tenth of the input demonstrated the presence of HDAC3 in both cell lines (lane 1).

(C) Histone deacetylation assay. Western blot analysis, with an anti-acetylated histone H4 antibody to detect deacetylase activity, of proteins bound by GST or GST-PPARγ. Complexes brought down by the two different GST fusion proteins were incubated with acetylated histone H4 (Lys 9) in the absence or presence of 0.5 mM 4-phenyl butyrate (4PB). Half of the input was used as a control (lane 4).

(D) Chromatin immunoprecipitation (ChIP) assays demonstrating binding of RB, PPARγ, or HDAC3 to the LPL promoter. Crosslinked chromatin from rosiglitazone-treated U2OS (upper panel) or SaOS (lower panel) cells was incubated with antibodies against RB (lane 2), PPARγ (lane 3), HDAC3 (lanes 4), or preimmune serum (lane 1). Immunoprecipitates were analyzed by PCR with primers specific for the human LPL promoter.

(E) Activity generated from the PPRE-TK-Luc reporter cotransfected in RB−/− MEFs with expression vectors for PPARγ, RB, or both together. Experiments were performed either without stimulation (cont) or in the presence of rosiglitazone (rosi), $10^{-7}$ M trichostatin A (TSA), or rosi and TSA. Fold induction of reporter activity by rosiglitazone relative to control or TSA, respectively, is indicated.

(F) Northern blot analysis showing expression of LPL and 36B4 mRNA in U2OS cells treated for 48 hr with vehicle (cont), rosiglitazone (rosi), TSA, or a combination of both. Fold induction is indicated.

(G) ChIP assays to analyze the presence of PPARγ, HDAC3, and acetylated histones on the human LPL promoter. Crosslinked chromatin from U2OS cells treated with vehicle (cont), rosiglitazone (rosi), TSA, or a combination of both was incubated with antibodies against PPARγ (lane 2), HDAC3 (lane 3), acetylated histone H4 (lane 4), or preimmune serum (Mock, lane 1). Immunoprecipitates were analyzed by PCR with primers specific for the human LPL promoter.

(H) GST pull-down assay demonstrating the disruption of the interaction between PPARγ and HDAC3 by TSA. COS cells were transfected with RB and HDAC3 and treated with rosiglitazone (rosi), $10^{-7}$ M TSA, or TSA and rosi. Extracts were incubated with GST or GST-PPARγ. Interaction of HDAC with GST-PPARγ increased in the presence of rosi and was diminished by the presence of TSA.

MDI and either of five chemically distinct HDAC inhibitors, i.e., suberoylanilide hydroxamic acid (SAHA), valproic acid (VA), 4PB, apicidin, or MS-276, accumulated significant amounts of lipids and differentiated into adipocytes (Figure 4A). Consistent with a stimulatory effect of HDAC inhibitors on PPARγ, the activity of the PPRE-TK-Luc reporter was dose dependently increased upon incubation with these structurally unrelated HDAC inhibitors (Figure 4B). 4PB and VA have been shown, respectively, to be able to bind (Samid et al., 2000) or activate (Lampen et al., 2001) PPARγ. Therefore, we analyzed the capacity of the various HDAC inhibitors to displace radiolabeled $^{3}$H-rosiglitazone bound to the GST-PPARγ DE fusion protein. 4PB ($K_i$ of 3 mM) and, to a lesser

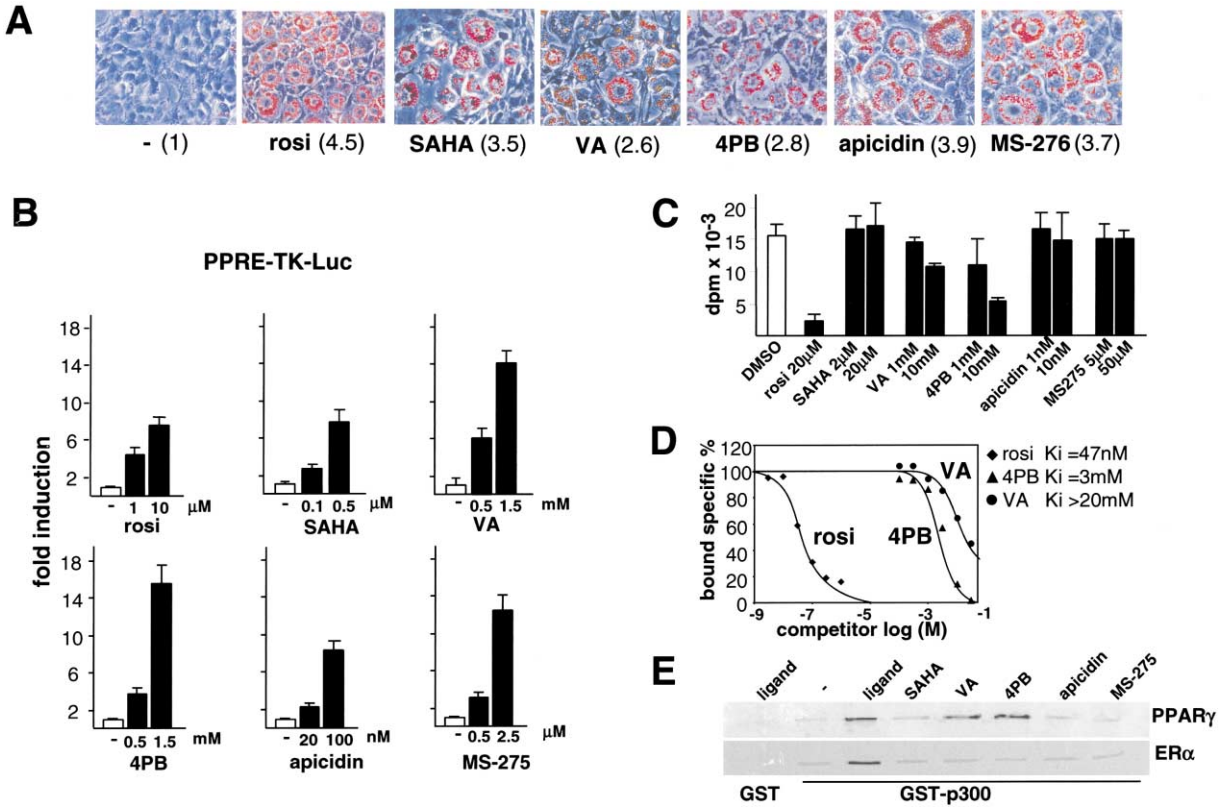


Figure 4. PPARγ Activity Is Restored in RB+/+ Cells in the Presence of HDAC Inhibitors

(A) Micrographs of confluent 3T3-L1 cells treated for 4 days with MDI differentiation mix or MDI, to which rosiglitazone (rosi), 0.2 μM SAHA, 1.5 mM VA, 1.5 mM 4PB, 50 nM apicidin, or 2.5 μM MS-275 was added. Cells were stained with Oil Red O. Quantification of red staining (Adobe Photoshop 6) is indicated.

(B) Activity of the PPRE-TK-Luc reporter transfected in NIH-3T3 cells, in the absence (white bar) or presence of increasing concentrations of rosiglitazone, SAHA, VA, 4PB, apicidin, or MS-275 (shaded bars).

(C) Radioligand displacement assay. Nonradioactive 4PB and VA compete, whereas SAHA, MS-275, and apicidin do not compete, with $^{3}$H-radiolabeled rosiglitazone for binding to GST-PPARγ. Values are expressed as disintegrations per minute. Radioactivity in the presence of cold rosiglitazone defines unspecific binding.

(D) Similar radioligand displacement assay, as in (C), performed with increasing concentrations of VA and 4PB. $K_i$ values of both compounds are indicated.

(E) Cofactor recruitment assay. SDS-PAGE electrophoresis showing in vitro-translated radiolabeled PPARγ or ERα retained by either GST or GST-p300 fusion protein upon incubation with vehicle, ligand (either estradiol or rosiglitazone at 1 μM), SAHA (5 μM), VA (5 mM), 4PB (5 mM), apicidin (1 μM), or MS-275 (5 μM).

extent, VA ($K_i > 20$ mM) were able to compete for binding with rosiglitazone (Figures 4C–4D), demonstrating that they are low-affinity PPARγ ligands. In contrast, SAHA, MS-275, and apicidin did not compete with $^{3}$H-rosiglitazone for binding to PPARγ (Figure 4C). In addition to this ligand binding assay, a cofactor recruitment assay was performed with these HDAC inhibitors, stipulating that direct PPARγ ligands should facilitate cofactor recruitment. Rosiglitazone stimulated the interaction of GST-p300 with PPARγ, whereas SAHA, apicidin, and MS-275 did not induce such an interaction (Figure 4E). 4PB and VA enhanced the recruitment of p300 to PPARγ (Figure 4E), confirming that they are PPARγ ligands. None of the HDAC inhibitors facilitated p300 docking to the estrogen receptor α (ERα; Figure 4E), indicating that binding of VA and 4PB to PPARγ was specific. In combination, these data prove that HDAC inhibitors, such as SAHA, apicidin, and MS-275, which do not bind to PPARγ, stimulate its proadipogenic activity by inhibiting the repressive PPARγ-RB-HDAC3 complex. Furthermore, in the case of VA and 4PB, both direct ligand activation of PPARγ and HDAC inhibition could contribute to their adipogenic activity.

The detection of a PPARγ-RB-HDAC3 protein complex on the promoter of well-established PPARγ targets in vivo, as well as the fact that the proadipogenic effects of PPARγ were blunted by the presence of RB, on the one hand, and stimulated by HDAC inhibitors, on the other hand, underscores the relevance of the repression of PPARγ by RB and HDAC3. Complexes involved in nuclear receptor-mediated transcriptional repression often contain HDACs (Nagy et al., 1997). The thyroid receptor, as does PPARγ, specifically recruits HDAC3 (Li et al., 2002). Participation of HDACs in the repressive activity of nuclear receptor is facilitated by the presence of other corepressors, such as the silencing mediator of retinoic and thyroid receptors (SMRT) or the nuclear receptor corepressor (N-CoR). Furthermore, corepressors such as SMRT and N-CoR are required for the activation of HDAC3 in such complexes (Guenther et al., 2001). It is therefore tempting to speculate that RB fulfills such a corepressor role for PPARγ.

The fact that ligand binding stimulates recruitment of RB by PPARγ suggests that RB, unlike most typical nuclear receptor corepressor complexes, might specifically reduce ligand-induced responses. The attenuation of the activity of ligand-bound PPARγ only occurs with hypophosphorylated, but not with hyperphosphorylated, RB. Under conditions where optimal PPARγ activity is required, such as during adipogenesis, RB is mainly phosphorylated and, hence, dissociates from PPARγ. The fact that the interaction of PPARγ and RB is regulated through both the status of PPARγ and RB actually allows fine-tuning of PPARγ. This so-called "double gating" of PPARγ activity, by both ligand binding to PPARγ and phosphorylation of RB, also allows distinct signaling pathways to convergently affect target gene expression.

These observations led us to hypothesize that PPARγ can exist in several complexes with distinct activity. First, PPARγ can occur as an inactive and unliganded receptor. Second, ligand-bound PPARγ can be transcriptionally repressed through complex formation with hypophosphorylated RB and HDAC3. Finally, ligand-bound PPARγ can, consequent to RB phosphorylation or HDAC inhibition, release RB and HDAC3 and actively recruit coactivators, enabling transcription. Hypophosphorylated RB can therefore be seen as an actual corepressor, which, unlike most corepressors, interacts with a ligand-bound receptor. Interestingly, recruitment of a corepressor to a ligand-bound receptor is not unique to PPARγ and RB, since a similar repression of ligand-induced receptor activation has been reported for repressor complexes, such as those coordinated by the receptor interacting protein (RIP140) (Cavailles et al., 1995; Treuter et al., 1998), the SMRT/HDAC1-associated repressor protein (SHARP) (Shi et al., 2001), the transcription intermediary factor 1 (TIF-1) (Beckstead et al., 2001), the metastasis-associated protein 1 corepressor (MTA) (Mazumdar et al., 2001), and the small heterodimer partner SHP (Johansson et al., 1999).

RB has been previously shown to facilitate the differentiation of preadipocytes and MEFs into adipocytes (Chen et al., 1996a; Classon et al., 2000; Higgins et al., 1996), which seems at odds with our results. This apparent paradox can be explained by a dual effect of RB in adipocyte differentiation. On the one hand, RB mediates the cell cycle arrest required for adipocyte differentiation (Higgins et al., 1996). Furthermore, it was suggested that enhanced transcriptional activation of C/EBP family members accounted for the adipogenic role of RB (Chen et al., 1996b), an observation questioned by the demonstration that C/EBP plays a subordinate role to PPARγ in adipogenesis (Rosen et al., 2002). Such a positive role of RB on cell cycle arrest and differentiation would, however, explain the decrease in adipogenesis observed in RB−/− MEFs by a standard differentiation protocol. On the other hand, RB can attenuate PPARγ activity by recruiting HDAC3 and, therefore, inhibit adipocyte differentiation. This explains the robust increase in lipid incorporation upon addition of PPARγ agonists to RB−/− MEFs, in which PPARγ is not inhibited by RB. The enhanced expression of PPARγ target genes and the stimulation of adipocyte differentiation observed upon HDAC inhibition is also consistent with such an inhibitory effect of RB-HDAC3 on PPARγ-mediated adipogenesis. Additional evidence for a negative role of RB is the predominance of phosphorylated and, thus, inactive RB during adipocyte differentiation (Figure 1E and Reichert and Eick, 1999). Finally, in vivo support for a more complex role of RB in adipocyte differentiation is provided by the observation that transgenic mice overexpressing RB show a significant decrease (by 43%) of paraovarian fat mass (Nikitin et al., 2001)

In summary, our data demonstrate that RB interacts with PPARγ and that this interaction results in the recruitment of HDAC3 to PPARγ target promoters. Similar to their role in the control of the transcription factor E2F1, RB and HDACs inhibit PPARγ activity, thereby modulating its effects on adipocyte differentiation.

## Experimental Procedures

### Materials

Rosiglitazone was provided by Carex S.A. (Strasbourg, France). $^{3}$H-radiolabeled rosiglitazone was purchased from ARC (St. Louis, MO). All chemicals, unless stated otherwise, were purchased from Sigma (St. Louis, MO). SAHA was purchased from Biomol (Buttler Pike, PA), and MS-275 and apicidin were from Calbiochem (San Diego, CA). Anti-PPARγ E-8 antibody was purchased from Santa Cruz Biotechnology (Santa Cruz, CA). The anti-RB antibody (G3-245) was from Pharmingen (San Diego, CA), and the acetylated histone H4 (Lys 9) peptide, anti-acetylated histone H4 (Lys 9) antibody, and anti-HDAC3 antibodies were from Upstate Biotechnology (Lake Placid, NY).

### Plasmids, Oligonucleotides, and Proteins

GST-RB, GST-p300, GST-PPARγ DE, UAS-TK-Luc, PPRE-TK-Luc, BD Gal4-PPARγ DE, cDNAs for aP2, LPL, 36B4, and the PPARγ and RB expression vectors were all described previously (Fajas et al., 2000; Rocchi et al., 2001). Oligonucleotides used in the ChIP assays to amplify the human LPL promoter are 5′-GGGCCCCCGGGTA GAGTGG-3′ and 5′-CACGCCAAGGCTGCTTATGTGACT-3′. $His_6$-tagged hPPARγ LBD (residues 203–477) was produced in *E. coli* BL21 (DE3) with the pET15b expression plasmid (Novagen, Madison, WI) and purified by immobilized metal ion affinity chromatography on a $Co^{2+}$-loaded HiTrap Chelating column (Pharmacia, Orsay, France), and then gel filtration chromatography was performed on a HiLoad Superdex 100 column (Pharmacia).

### Cell Culture, Protein Extracts, and Transfections

MEFs and 3T3-L1, U2OS, and SaOS cells (ATCC, Manassas, VA) were grown in DMEM with 10% fetal calf serum. In some differentiation studies MDI (0.5 mM 3-Isobutyl-1-methylxanthine, 10 μg/ml insulin, and 1 μM dexamethasone) was added for 2 days. From day 3 on, cells were incubated with 10 μg/ml insulin, and $10^{-6}$ M rosiglitazone was added when stated. Oil Red O staining (Rocchi et al., 2001) and nuclear and whole-cell extracts were prepared as described. Lipofectamine (Life Technologies, Rockville, MD) was used to transfect cells, and luciferase and β-gal activity was measured as described (Rocchi et al., 2001).

### Pull-Down, Coimmunoprecipitation, Chromatin Immunoprecipitation (ChIP), and Deacetylation Assays

In vitro translation of pSG5-PPARγ was performed with $^{35}$S-methionine (Amersham, Orsay, France) in a TNT-coupled reticulocyte lysate (Promega, Madison, WI). Pull-down, immunoprecipitation assays and ChIP assays were performed as described (Fajas et al., 2002). Histone deacetylation assays were performed by incubating GST-bound or GST-PPARγ-bound proteins from nuclear extracts with 2 μg of acetylated histone H4 for 3 hr at 21°C in HDAC buffer (10 mM Tris-Hcl [pH 8] and 150 mM NaCl in 50% glycerol). Histones were then separated in SDS-PAGE, electrotransfered, and blotted with anti-acetylated histone H4 (Lys9) antibody.

### Protein and RNA Expression

SDS-PAGE and electrotransfer were performed as described (Rocchi et al., 2001). The membranes were blocked overnight in blocking buffer (20 mM Tris, 100 mM NaCl, 1% Tween 20, and 10% skimmed

milk). Filters were first incubated for 4 hr at 21°C with primary antibody and then for 1 hr at 21°C with a peroxidase conjugate secondary antibody. The complex was visualized with 4-chloro-1-naphtol. RNA isolation, reverse transcription, and multiplex RT-PCR (Hansen et al., 1999) or northern blot hybridization (Rocchi et al., 2001) were performed as described.

### Radioligand Binding Assay

GST-PPARγ fixed on Sepharose beads was incubated for 4 hr at 4°C in 10 mM Tris (pH 8), 50 mM KCl, and 1 mM DTT with 5 nM $^{3}$H-rosiglitazone (1.4–220 nM for saturation analysis) in the absence or presence of either cold rosiglitazone or the indicated concentrations of HDAC inhibitors. This was followed by filtration on Whatman GF/C filters.

### Acknowledgments

C. Sardet, J.M. Blanchard, and W.M. Yang are acknowledged for the gift of materials, and P. Chambon is acknowledged for discussions. R.R. was supported by H. Batliner. This work was supported by grants of CNRS, INSERM, Hôpital Universitaire de Strasbourg, ARC, ARERS, an NIH Program project (1 P01-DK59820-01), and the EU RTD program (QLG1-CT-1999-00674 and QLRT-2001-00930).

Received: December 12, 2001
Revised: October 7, 2002

### References

Beckstead, R., Ortiz, J.A., Sanchez, C., Prokopenko, S.N., Chambon, P., Losson, R., and Bellen, H.J. (2001). Bonus, a *Drosophila* homolog of TIF1 proteins, interacts with nuclear receptors and can inhibit betaFTZ-F1-dependent transcription. Mol. Cell *7*, 753–765.

Brehm, A., Miska, E.A., McCance, D.J., Reid, J.L., Bannister, A.J., and Kouzarides, T. (1998). Retinoblastoma protein recruits histone deacetylase to repress transcription. Nature *391*, 597–601.

Cavailles, V., Dauvois, S., L'Horset, F., Lopez, G., Hoare, S., Kushner, P.J., and Parker, M.G. (1995). Nuclear factor RIP140 modulates transcriptional activation by the estrogen receptor. EMBO J. *14*, 3741–3751.

Chen, P., Riley, D.J., Chen, Y., and Lee, W. (1996a). Retinoblastoma protein positively regulates terminal adipocyte differentiation through direct interaction with C/EBPs. Genes Dev. *10*, 2794–2804.

Chen, P.L., Riley, D.J., Chen, Y., and Lee, W.H. (1996b). Retinoblastoma protein positively regulates terminal adipocyte differentiation through direct interaction with C/EBPs. Genes Dev. *10*, 2794–2804.

Choi, H., Lee, J., Park, J., and Lee, Y. (2002). Trichostatin A, a histone deacetylase inhibitor, activates the IGFBP-3 promoter by upregulating Sp1 activity in hepatoma cells: alteration of the Sp1/Sp3/HDAC1 multiprotein complex. Biochem. Biophys. Res. Commun. *296*, 1005.

Classon, M., Kennedy, B.K., Mulloy, R., and Harlow, E. (2000). Opposing roles of pRB and p107 in adipocyte differentiation. Proc. Natl. Acad. Sci. USA *97*, 10826–10831.

Fajas, L., Debril, M.B., and Auwerx, J. (2001). Peroxisome proliferator-activated receptor-gamma: from adipogenesis to carcinogenesis. J. Mol. Endocrinol. *27*, 1–9.

Fajas, L., Landsberg, R.L., Huss-Garcia, Y., Sardet, C., Lees, J.A., and Auwerx, J. (2002). E2Fs regulate adipogenesis. Dev. Cell *3*, 39–49.

Fajas, L., Paul, C., Zugasti, O., Le Cam, L., Polanowska, J., Fabbrizio, E., Medema, R., Vignais, M.L., and Sardet, C. (2000). pRB binds to and modulates the transrepressing activity of the E1A-regulated transcription factor p120E4F. Proc. Natl. Acad. Sci. USA *97*, 7738–7743.

Guenther, M.G., Barak, O., and Lazar, M.A. (2001). The SMRT and N-CoR corepressors are activating cofactors for histone deacetylase 3. Mol. Cell. Biol. *21*, 6091–6101.

Hansen, J.B., Petersen, R.K., Larsen, B.M., Bartkova, J., Alsner, J., and Kristiansen, K. (1999). Activation of peroxisome proliferator activated receptor γ bypasses the function of the retinoblastoma protein in adipocyte differentiation. J. Biol. Chem. *274*, 2386–2393.

Higgins, C., Chatterjee, S., and Cherington, V. (1996). The block of adipocyte differentiation by a C-terminally truncated, but not by full-length, simian virus 40 large tumor antigen is dependent on an intact retinoblastoma susceptibility protein family binding domain. J. Virol. *70*, 745–752.

Johansson, L., Thomsen, J.S., Damdimopoulos, A.E., Spyrou, G., Gustafsson, J.A., and Treuter, E. (1999). The orphan nuclear receptor SHP inhibits agonist-dependent transcriptional activity of estrogen receptors ERalpha and ERbeta. J. Biol. Chem. *274*, 345–353.

Lampen, A., Carlberg, C., and Nau, H. (2001). Peroxisome proliferator-activated receptor delta is a specific sensor for teratogenic valproic acid derivatives. Eur. J. Pharmacol. *431*, 25–33.

Li, J., Lin, Q., Wang, W., Wade, P., and Wong, J. (2002). Specific targeting and constitutive association of histone deacetylase complexes during transcriptional repression. Genes Dev. *16*, 687–692.

Magnaghi-Jaulin, L., Groisman, R., Naguibneva, I., Robin, P., Lorain, S., Le Villain, J.P., Troalen, F., Trouche, D., and Harel-Bellan, A. (1998). Retinoblastoma protein represses transcription by recruiting a histone deacetylase. Nature *391*, 601–605.

Mazumdar, A., Wang, R.A., Mishra, S.K., Adam, L., Bagheri-Yarmand, R., Mandal, M., Vadlamudi, R.K., and Kumar, R. (2001). Transcriptional repression of oestrogen receptor by metastasis-associated protein 1 corepressor. Nat. Cell Biol. *3*, 30–37.

Nagy, L., Kao, H.K., Chakravarti, D., Lin, R.J., Hassig, C.A., Ayer, D.E., Schreiber, S.L., and Evans, R.M. (1997). Nuclear receptor repression mediated by a complex containing SMRT, mSin3A, and histone deacetylase. Cell *89*, 373–380.

Nikitin, A., Shan, B., Flesken-Nikitin, A., Chang, K.H., and Lee, W.H. (2001). The retinoblastoma gene regulates somatic growth during mouse development. Cancer Res. *61*, 3110–3118.

Reichert, M., and Eick, D. (1999). Analysis of cell cycle arrest in adipocyte differentiation. Oncogene *18*, 459–466.

Richon, V., Lyle, R.E., and McGehee, R.E.J. (1997). Regulation and expression of retinoblastoma proteins p107 and p130 during 3T3–L1 adipocyte differentiation. J. Biol. Chem. *272*, 10117–10124.

Rocchi, S., Picard, F., Vamecq, J., Gelman, L., Potier, N., Zeyer, D., Dubuquoy, L., Bac, P., Champy, M.F., Plunket, K.D., et al. (2001). A unique PPARgamma ligand with potent insulin-sensitizing yet weak adipogenic activity. Mol. Cell *8*, 737–747.

Rosen, E.D., Hsu, C.H., Wang, X., Sakai, S., Freeman, M.W., Gonzalez, F.J., and Spiegelman, B.M. (2002). C/EBPalpha induces adipogenesis through PPARgamma: a unified pathway. Genes Dev. *16*, 22–26.

Rosenbaum, S.E., and Greenberg, A.S. (1998). The short- and long-term effects of tumor necrosis factor-alpha and BRL 49653 on peroxisome proliferator-activated receptor (PPAR)gamma2 gene expression and other adipocyte genes. Mol. Endocrinol. *12*, 1150–1160.

Samid, D., Wells, M., Greene, M.E., Shen, W., Palmer, C.N., and Thibault, A. (2000). Peroxisome proliferator-activated receptor gamma as a novel target in cancer therapy: binding and activation by an aromatic fatty acid with clinical antitumor activity. Clin. Cancer Res. *6*, 933–941.

Schoonjans, K., Peinado-Onsurbe, J., Lefebvre, A.M., Heyman, R., Briggs, M., Deeb, S., Staels, B., and Auwerx, J. (1996). PPARα and PPARγ activators direct a tissue-specific transcriptional response via a PPRE in the lipoprotein lipase gene. EMBO J. *15*, 5336–5348.

Shao, D., and Lazar, M.A. (1997). Peroxisome proliferator activated receptor γ, CCAAT/enhancer binding protein α, and cell cycle status regulate the commitment to adipocyte differentiation. J. Biol. Chem. *272*, 21473–21478.

Shi, Y., Downes, M., Xie, W., Kao, H.Y., Ordentlich, P., Tsai, C.C., Hon, M., and Evans, R.M. (2001). Sharp, an inducible cofactor that integrates nuclear receptor repression and activation. Genes Dev. *15*, 1140–1151.

Treuter, E., Albrektsen, T., Johansson, L., Leers, J., and Gustafsson, J.A. (1998). A regulatory role for RIP140 in nuclear receptor activation. Mol. Endocrinol. *12*, 864–881.